Real-Time Staircase Cyclic Voltammetry Fourier Transform Electrochemical Impedance Spectroscopic Studies on Underpotential Deposition of Lead on Gold

Byoung-Yong Chang, Eunshil Ahn, and Su-Moon Park*

Department of Chemistry and Center for Integrated Molecular Systems, Pohang University of Science and Technology, Pohang, Gyeongbuk 790-784, Korea

Received: July 7, 2008; Revised Manuscript Received: August 5, 2008

We report results of detailed studies on the underpotential deposition of lead (Pb UPD) and effects of specifically adsorbed halide anions on the UPD reaction at polycrystalline gold electrodes employing real-time staircase cyclic voltammetry Fourier transform electrochemical impedance spectroscopy (SCV-FTEIS). Potential shifts observed during the Pb UPD in the presence of halide ions are partially attributed to the chemical interaction of halide ions with Pb^{2+} as well as the physical obstruction by the preadsorbed halide ions. More importantly, the presorbed halides, on the top of which Pb^{2+} ions are adsorbed, form a pseudocapacitor on the gold surface, and its electrical discharge leads to the Pb UPD. Real-time SCV-FTEIS measurements in a chloride solution without Pb^{2+} reveal that the voltammetric currents arise from charging both the double-layer and pseudocapacitors formed due to the presorption of halide ions at the surface, indicating that the capacitors formed upon adsorption of halide ions on the electrode surface play a critical role in the Pb UPD.

Introduction

Underpotential deposition (UPD) of a metal, which occurs at potentials more positive than their equilibrium potentials for the bulk deposition,[1,2] is very important in determining the quality of electrodeposited metals. Generally, up to a monolayer is formed in this way until three-dimensional clusters begin to grow, leading to the bulk deposition. The UPD is observed when the metal adsorbate has a stronger affinity to the substrate than the deposited metal. The underpotential is estimated by the Kolb−Gerischer relation for the metal UPD on a foreign polycrystalline substrate[3]

$$\Delta E = \frac{1}{2}\Delta\Phi \tag{1}$$

where ΔE is the difference between the potentials for the UPD and the bulk deposition in V and $\Delta\Phi$ is the difference between the work functions of the metal and the substrate electrode in electron volts.[3] The UPD is so sensitive to the surface of the substrate electrode that the extent and the potentials for UPD depend on the surface states such as facets or defects of the substrate. Such effects seem to get averaged on a polycrystalline surface. The anion presorption on a substrate is also one of the crucial factors affecting the UPD process.[4] Anions presorbed are expected to exert considerable influences on the UPD due to their cooperative and competitive effects. The Pb UPD has been studied extensively on single crystalline substrates such as Au(111),[5a−c] Au(100),[5a,d,e] and Au(110),[5a] as well as polycrystalline gold.[6a−c]

The studies on UPDs have been conducted mostly using traditional electrochemical and nontraditional surface analytical techniques.[7,8] Traditional electrochemical techniques such as cyclic voltammetry and galvanostatic experiments,[5,6a] as well as other complementary experiments including scanning tunneling microscopy,[5] impedance measurements,[7] and electrochemical quartz crystal microbalance measurements,[6b,c] have been employed for the studies. These studies have mainly addressed the thermodynamics,[6a,b] kinetics,[7a] electrosorption valency,[6c,d] and structural[5c] aspects of the Pb UPD on various substrates. Many of these studies addressed primarily how and where on the crystal facets of the substrate the UPD takes place rather than the nature of the interaction.

Traditional impedance measurements provided information on a steady state system,[5] which is hardly relevant to transient electron transfer reactions. Recently, Bondarenko et al. conducted potentiodynamic electrochemical impedance spectroscopic (PDEIS) experiments to study the Pb UPD on polycrystalline gold electrodes during potential scans.[9a,b] While this technique was claimed to provide information on the Pb UPD in nonstationary states, the scan rate used, 2 mV/s, appeared too slow to record truly nonstationary impedance signals during the UPD reaction. The scan rate must be slow enough to keep the potential virtually constant during the period of one wavelet in this method.[9c,10] We have recently developed a staircase cyclic voltammetry Fourier transform electrochemical impedance spectroscopy (SCV-FTEIS) technique, by which EIS measurements are made in real time, while the SCV experiments are being recorded.[11] Thus, EIS data are obtained at a desired bias potential even at fast scan rates up to a few volts per second when only high frequency information is needed.[12] In fact, we were not the first in using the FT to interpretations of currents obtained upon application of periodic waves such as saw tooth, square, or sinusoidal waves to electrochemical cells.[13] However, the authors of these studies[13] focused on presenting the results in voltammetric rather than impedance formats by employing *IV* curves of specific harmonic frequencies, which they called FT voltammetry. The difference between SCV-FTEIS and FT voltammetry is in how the same results are visualized: each step period was transformed to visualize impedance profiles in the SCV-FTEIS, whereas periodic characteristics were extracted for the construction of voltammograms in the FT voltammetry. We have also attempted to use other types of waves for SCV-FTEIS as had been in our studies,[13] but we found the staircase wave to be the most efficient. As a result, the technique allows

* To whom correspondence should be addressed. E-mail: smpark@postech.edu. Phone: +82-54-279-2102. Fax: +82-54-279-3399.

10.1021/jp805960j CCC: $40.75
Published on Web 10/01/2008

the information on both thermodynamic and kinetic parameters, as well as on electrical properties of the double-layer formed at the electrode/electrolyte interface, to be obtained on an electrochemical reaction in real time by a single pass of an SCV experiment, as we already pointed out in an earlier publication.[12] The kinetic parameters include both electron transfer (the exchange rate constant and the transfer coefficient) and mass transfer kinetics (diffusion). The instrumentation, however, is rather simple as has been described elsewhere in detail with its power primarily coming from the FT analysis.[11,12]

In the present work, we report results obtained from our studies on the Pb UPD on polycrystalline gold surfaces in the presence of halide ions using the SCV-FTEIS experiments. The information on the electrode/electrolyte interface obtained by real-time SCV-FTEIS measurements during the UPD reaction allowed the UPD process to be described more clearly. This is because the important information is contained in the high frequency domain of the currents observed during the UPD process.

Experimental Section

The UPD reactions of $Pb(NO_3)_2$ ions were studied on polycrystalline gold (Au) electrodes in 0.10 M HNO_3 solutions containing 12 mM $Pb(NO_3)_2$ with or without 10 mM NaCl, KCl, and KBr added. Double-distilled, deionized water was used for the preparation of all solutions. $Pb(NO_3)_2$ (98%), NaCl (99.999%), KCl (99.99%), and KBr (99%), which were all obtained from Aldrich, and HNO_3 (60%) obtained from Matsunoen Chemicals Ltd. were used as received.

A single-compartment cell, which housed a gold disk working electrode with its diameter of 1.6 mm (geometric area = 0.020 cm^2) embedded in a Teflon rod, a platinum gauze counter electrode, and a homemade Ag|AgCl (in saturated KCl) reference electrode, was used for the electrochemical measurements. The working electrode was polished to a mirror finish successively with alumina slurries of 14.5 μm down to 0.05 μm and sonicated in doubly distilled water just before it was used.

The SCV-FTEIS measurements were conducted using a homemade fast-rise potentiostat, which had a rise time of <50 ns/V. Ascending or decending staircase potential waves whose step height was 7.5 mV were generated by an Agilent 33120 Arbitrary Waveform Generator and applied to the working electrode at every 75 ms in a potential range of 0.25 to −0.35 V; this corresponded to a scan rate of 100 mV/s for the staircase voltammetric experiment (vide infra). Scan rates up to 500 mV/s were also used by adjusting the step period to 15 ms when needed. A series of ascending or descending voltage steps applied and currents obtained thereof were acquired at a rate of 50k samples/s using a National Instrument NI-5922 high-speed data acquisition system of a 24-bit resolution. The data acquisition system was interfaced to a Pentium-4 PC through its PCI slot.

After the data acquisition, both the potential and current data obtained from each potential step were segmented into a packet. A staircase cyclic voltammogram was obtained by connecting the so-called pseudocurrents at each base potential, which were calculated by dividing the charge obtained by integrating the chronoamperometric current recorded during each potential step for the step period (75 ms) in each data segment; the SCVs thus constructed gave the same features as those of the cyclic voltammograms recorded at the scan rate obtained by dividing the step height by the step period.[14] Impedances were then computed by first transforming the derivative signals of the potential and current data into the frequency domain by a discrete Fourier transform (DTFT) method[11a] with frequencies ranging from $1/t_{total}$ (13.3 Hz) to $1/(2\Delta t)/2$ (12.5 kHz), where Δt = 1/(sampling rate), followed by dividing the alternating current voltages by the alternating currents obtained thereof.[11] The Nyquist theorem states that the frequency would range between $1/(2\Delta t)$ and $1/t_{total}$; however, the upper frequency limit was set at $1/(2\Delta t)/2$ because of high-frequency noise encountered. The calculations were carried out using a Matlab program, and circuit simulations were conducted to fit the observed data using the EG & G's ZSimpWin program. Details of the related theory of the SCV-FTEIS and its experimental validation have been published elsewhere.[12]

Results and Discussion

Lead UPD reactions have been studied under a variety of experimental conditions in aqueous solutions. Kirowa-Eisner et al.[6b] showed that the Pb UPD reaction can be an electron or a mass transfer limited process depending on experimental conditions. At the polycrystalline gold electrode, the reaction was reversible with two UPD peaks observed between the sweep rates of 40 and 400 mV/s, and the CV peak shapes could be explained in the framework of the Frumkin isotherm with appropriate interaction parameters.[9a] In our present work, we opted to conduct the study such that mass transfer effects need not be taken into accounts by running experiments in a relatively concentrated Pb^{2+} solution of 12 mM in the presence and absence of halides at a reasonably fast sweep rate, 100 mV/s.

Figure 1 shows a series of SCVs[12,14] obtained at scan rates between 100 and 500 mV/s in a solution containing 12 mM $Pb(NO_3)_2$ and 0.1 M HNO_3, with (a) 10 mM NaCl or (b) KBr present at a polycrystalline gold disk electrode. Sharp UPD peaks are usually assigned to those taking place at different crystal facets exposed to the solution;[15,16] both peaks observed here are not as sharp as typical UPD peaks observed at a single crystal such as Au(110) because sharp peaks observed at various crystal facets and defect sites are convoluted. The same features have been reported in previous studies at polycrystalline gold electrodes.[5e,6a,9] The formal potential ($E^{\circ\prime}$) taken from the average of peak potentials of the forward and reversal scans of about of 0.05 V in Figure 2 is close the potential predicted by the Kolb−Gerischer relation, eq 1, which is 0.02 V, from the standard reduction potential for bulk deposition (−0.33 V vs Ag|AgCl in saturated KCl) and the differences in work functions of Au (5.1 eV) and Pb (4.4 eV). Thus, our observation is in good agreement with the prediction. As pointed out, the second UPD peak at about −0.22 V must be that taking place at the sites where the first UPD did not occur.

We first examined effects of halide ions on the Pb UPD. Figure 2 shows SCVs recorded in the presence and absence of NaCl, KCl, and KBr, in which two current peaks became more distinctive and the UPD peak potentials shifted to more negative values in the presence of halide ions. Also, the potential shifts for both peaks are larger for the bromide ion than for the chloride. On the contrary, almost no effects of cations were observed. These observations may be explained by a few reasons. First, the presorbed halide ions might *physically* obstruct the Pb reduction as Pb^{2+} ions are adsorbed on the top of specifically adsorbed halides,[17] which may make the Pb UPD more difficult. The specific adsorption increases in the order of $F^- < Cl^- < Br^- < I^-$ with the same order of the free energy for adsorption,[17b] which is in good agreement with the shifts in voltammetric peaks during the Pb UPD. It appears that the specifically adsorbed halide ions lead to a thermodynamically higher energy for the Pb UPD, but its kinetics may become

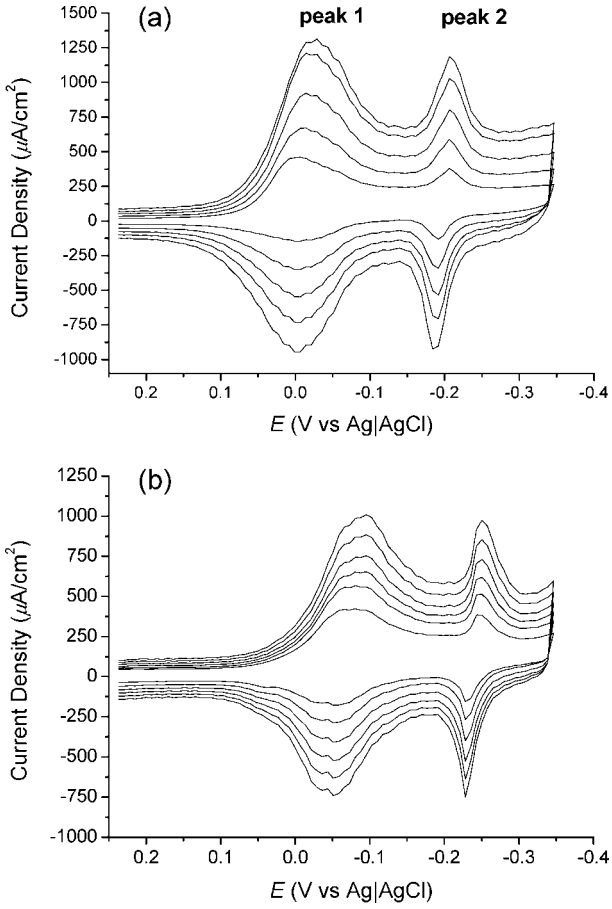

Figure 1. SCVs obtained for Pb UPD in a solution containing 12 mM $Pb(NO_3)_2$ and 0.10 M HNO_3 at a polycrystalline gold disk electrode in the presence of: (a) 10 mM NaCl at scan rates of 100, 200, 300, 400, and 500 mV/s and (b) 10 mM KBr at scan rates of 100, 150, 200, 250, 300, and 350 mV/s.

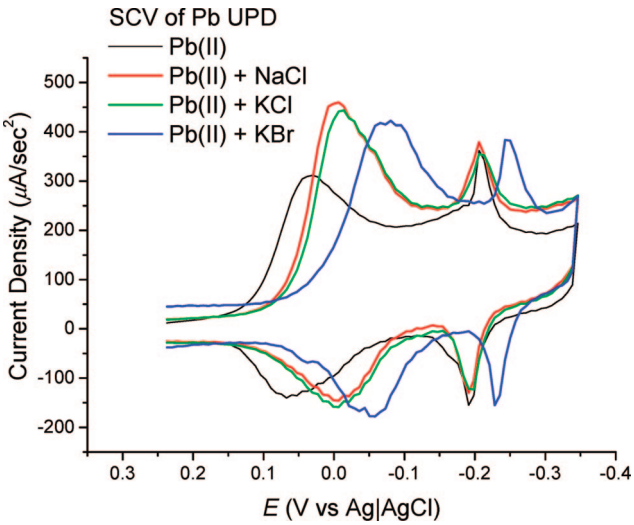

Figure 2. SCVs obtained for Pb UPD in a solution containing 12 mM $Pb(NO_3)_2$ and 0.10 M HNO_3 in the absence and presence of 12 mM NaCl, KCl, or KBr. The scan rate was 100 mV/s.

faster as shown by larger current densities due to their electron shuttling capabilities from the electrode to Pb^{2+}.

Another reason for the potential shifts could be due to the *chemical* interaction between presorbed halide and Pb^{2+} ions. When Pb^{2+} is chemically bound to halide ions forming a complex or a precipitate, it would become energetically more difficult to be reduced by as much as its bond energy with the halide. Accordingly, the reduction potential would shift in a negative direction to a degree that depends on the formation constant and the anion concentration. Lead ions form precipitates (PbX_2) and/or complexes ($PbX_n^{(n-2)-}$) with halides depending on halide concentrations, which should be broken before Pb^{2+} is reduced. The solubility product constants are 1.2×10^{-5} and 6.6×10^{-6}, respectively, for $PbCl_2$ and $PbBr_2$.[18] The potential shift, ΔE, for this reaction can be calculated from the equation shown below[19]

$$\Delta E = -\frac{RT}{nF}\ln K_C - \frac{RT}{nF}p \ln C_X^* + \frac{RT}{nF}\ln\frac{m_M}{m_X} \qquad (2)$$

where K_C is the formation constant, p is the stoichiometric coefficient, C_X^* is the concentration of halide ions, and m_M and m_X are the mass-transfer coefficients of Pb^{2+} and the lead halide, respectively. The potential shifts calculated using eq 2 are about -27.2 and -34.9 mV, respectively, for Cl^- and Br^-, assuming $m_M \approx m_X$. These values are too small to explain the observed potential shifts of -45 and 110 mV. Complexes are not likely to be formed due to relatively low concentrations of the ligands although the formation constants are larger than those of precipitates by about 2 orders of magnitude.[20]

We thus need to consider another mechanism to explain the relatively large potential shifts and ran the real-time SCV-FTEIS experiments to elucidate the effects. Figure 3 shows (a) an SCV and (b) a few Nyquist plots for the impedance data obtained at a few potentials labeled on the SCV during the potential scan. All the impedance data obtained in the potential range, in which the Pb UPD was observed, were fitted rather well with both the equivalent circuits shown in Figure 4 with χ^2 values in the order of low 10^{-4} in a potential range of 0.1−0.35 V. The equivalent circuit shown in Figure 4a appears similar to that used for the Bi UPD[10a] but is less complicated due perhaps to the experimental conditions, under which the reaction is not the mass transfer limited and is thus surface confined. The circuit in Figure 4b is the same as that for Pb UPD used by Bondarenko et al.[9b] except that the Warburg element is missing for the same reason stated above. Thus, the electrochemistry of the Pb UPD can be described as an interfacial phenomena depicted by the equivalent circuits shown in parts a and b of Figure 4. More will be discussed below on the relevance of the two circuits.

The circuit shown in Figure 4a shows a parallel connection of the electrical double-layer capacitor, C_{dl}, with the pseudocapacitor, C_φ; C_φ can be charged or discharged via a potential dependent faradaic process. Thus, the electron transfer to adsorbed Pb^{2+} takes place via R_{p2} while C_φ is being charged. Note that there is no Warburg impedance or contribution from mass transfer. This is consistent with the fact that the UPD occurs on a monolayer or submonolayer scale by electrochemical reduction of adsorbed metal ions and is thus interpreted in terms of the capacitive behavior. Such a capacitive behavior is also demonstrated by the scan rate dependencies of the peak currents of CVs as displayed in Figure 5. The currents of both CV peaks are directly proportional to the scan rate (v), not $v^{1/2}$, with a zero intercept. The capacitances obtained from the equation, $i_p = Cv$,[19] are listed in Table 1, which are shown to be heavily affected by the anions present in the solution.

The R_p values, which are charge-transfer resistances dependent on the polarized potential, are plotted in the form of admittances (or conductance, $1/R_p$) in Figure 6. The potentials at maximum admittances are in excellent agreement with those of maximum SCV currents, and the admittance is increased when the halides are present. This supports the statement on an

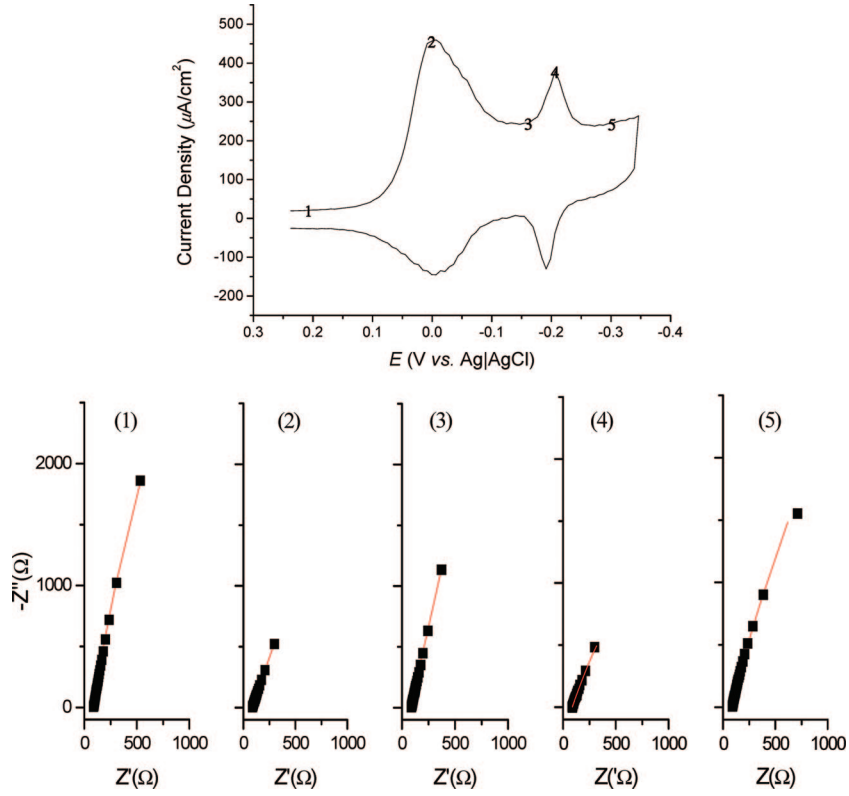

Figure 3. An SCV (top) for the Pb UPD in the prescence of 12 mM NaCl and a few typical Nyquist plots for the impedance data obtained from concurrent FTEIS measurements while the potential is scanned at 100 mV/s. The impedance data were obtained at the potentials marked on the SCV. The dotted points represent the experimental data, and the solid lines are the fitted curves according to the equivalent circuit shown in Figure 4a.

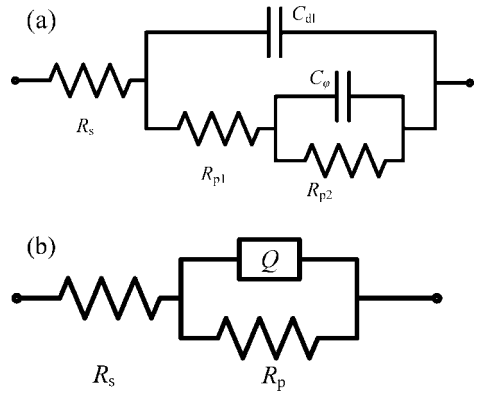

Figure 4. (a) Equivalent circuit used for fitting the impedance data shown in Figure 3 and (b) a simplified equivalent circuit for part a. Both provided good simulation results for the data shown in Figure 3 as well as other impedance data.

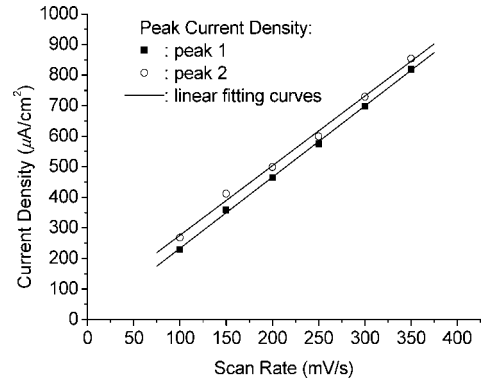

Figure 5. The peak current vs scan rate plots for peaks 1 and 2 in Figure 1b.

electron shuttling role of the adsorbed anions mentioned above; the anions render thermodynamics of UPD less favorable but enhance the kinetics of the Pb UPD in the order of none < Cl^- < Br^-. We thus postulate that both Cl^- and Br^- exert influences on the first stage of the UPD corresponding to the first peak current while the second stage corresponding to the second peak current is affected only by Br^- as can be seen in Figures 2 and 6.

Two types of capacitive behaviors include: the double-layer capacitance, C_{dl}, formed by the alignment of counterions along the charged electrode surface, and the pseudocapacitance, C_φ, formed by the adsorbed electroactive species.[21] Charging a double-layer capacitor is a nonfaradaic process, whereas it is faradaic for a pseudocapacitor. As shown in Figure 7a, the double-layer capacitances observed here are much larger than a typical double-layer capacitance of 10 to 20 $\mu F/cm^2$ at a normal electrified interface with no specific adsorption. Both the double-layer and pseudocapacitances are shown to change in a way similar to how the *IV* curves do as can be seen in Figures 1 and 2 as well as in parts a and b of Figure 7. Both C_{dl} and C_φ were obtained by fitting the impedance data to the equivalent circuit shown in Figure 4a. The double-layer charging currents are influenced by the specifically adsorbed anions in the system. In a positive potential region before the electrochemical activation starts, the capacitance values are determined only by the adsorbed anions regardless of the potential. Thus, Figure 7a shows that the capacitance increases from 70 to 120 and 160 $\mu F/cm^2$, respectively, when Cl^- and Br^- are added before the UPD reaction starts, to a few hundred microfarads. As soon as the UPD reaction is initiated, the capacitance increases rapidly because more Pb^{2+} ions are adsorbed on the top of the presorbed anions as the potential becomes negative.

TABLE 1: Total Effective Capacitances Obtained from the Scan Rate Dependencies of the CV Peak Currents ($i_p = Cv$) Shown in Figure 5 and by the FTEIS Method Using Eq 7 and Pseudocapacitances Obtained from the Langmuir Model

	C_{eff} from scan rate dependency of CV peak currents, mF/cm^2		C_{eff} from the FTEIS method, mF/cm^2		C_φ, pseudocapacitances from figure 8, mF/cm^2	
	peak 1	peak 2	peak 1	peak 2	peak 1	peak 2
no additive	1.33	1.81	1.30	1.81	0.32	0.50
NaCl	2.14	2.26	2.15	2.26	0.61	0.61
KCl	2.43	2.01	2.43	2.01	0.58	0.52
KBr	1.92	2.16	1.92	2.16	0.46	0.80

In other words, both the double-layer and pseudocapacitors are induced to form.

The pseudocapacitances resulting from adsorbed ions have been studied in the framework of Langmuir as well as Frumkin isotherms.[22] For the Langmuir isotherm, both the fractional coverage (θ) by the adsorbate and the resulting pseudocapacitance (C_φ) are related to the potential according to

$$\theta = \frac{KC\exp(-nEF/RT)}{[1 + KC\exp(-nEF/RT)]} \quad (3)$$

$$C_\varphi = nq\left(\frac{\partial\theta}{\partial E}\right) = \frac{n^2qF}{RT}\frac{KC\exp(-nEF/RT)}{[1 + KC\exp(-nEF/RT)]^2} \quad (4)$$

Here K is the equilibrium constant, and C is the concentration of the adsorbate in solution. We fitted the observed pseudocapacitance shown in Figure 7b for Pb^{2+} in the KCl solution to eq 4, and the results are shown in Figure 8. The C_φ vs E curve is almost perfectly fitted to eq 4. However, the n values (apparent number of electrons transferred for the UPD reactions) obtained from the fitting were 0.75 and 2.65 for the first and second UPD peaks instead of the expected value 2. This suggests that the Pb UPD does not take place by a single-step 2-electron transfer. The reaction perhaps goes through intermediate steps. Furthermore, pseudocapacitances (C_φ) obtained from the Langmuir model are only fractions (0.25−0.31) of the total effective capacitances (C_{eff}) obtained from CV peak currents or by the impedance measurements to be described below (see Table 1). These results suggest that the Pb^{2+} adsorption first follows the Langmuir isotherm when a large surface is available for adsorption until the Frumkin mechanism takes over when the Pb^{2+} coverage reaches about $^1/_4$−$^1/_3$ of the total area available for Pb UPD via the Langmuir model. At this point, the adsorbed Pb ions should start to interact with each other, and the Frumkin model takes over.

The Langmuir model assumes no interactions between the adsorbed species and, thus, does not explain interionic interactions that might be present; we thus employed the Frumkin isotherm to obtain Frumkin parameters. The Frumkin isotherm takes the lateral interionic interactions between adsorbates into account.[6b,23,24] As no mathematical expression is available for C_φ as a function of potential in the Frumkin model,[23] we used only two known relations to estimate Frumkin parameters

$$C_{\varphi,max} = \frac{n^2qF}{4RT}\frac{1}{1 + f/4} \quad (5)$$

$$W_{1/2} \cong \frac{90.2 + 27.7f}{n} \quad (6)$$

where f is the Frumkin parameter, nq is the charge that would have been consumed for the formation of a full monolayer, and $W_{1/2}$ is the bandwidth of the C_φ vs E plot. A negative f value indicates an attractive interaction between neighboring adsorbed ions/molecules on the surface, while a positive f value a repulsive interaction.

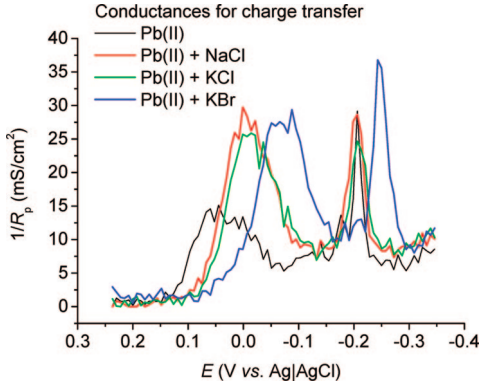

Figure 6. The conductance obtained from $1/R_p$ plotted as a function of potential in various solutions.

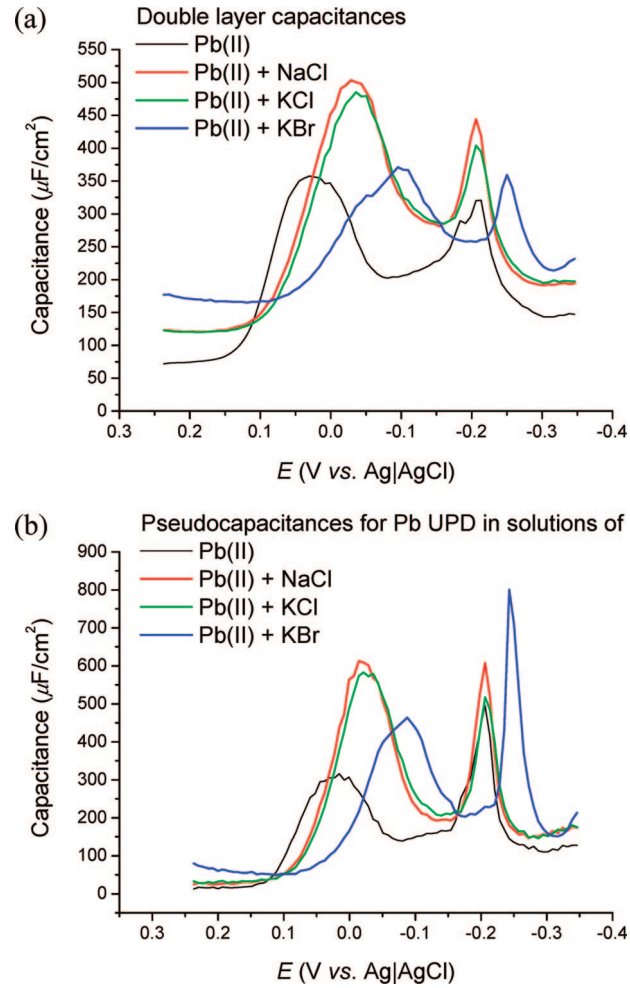

Figure 7. (a) The double-layer capacitances and (b) the pseudocapacitances obtained by fitting the impedance data to the equivalent circuit shown in Figure 4a.

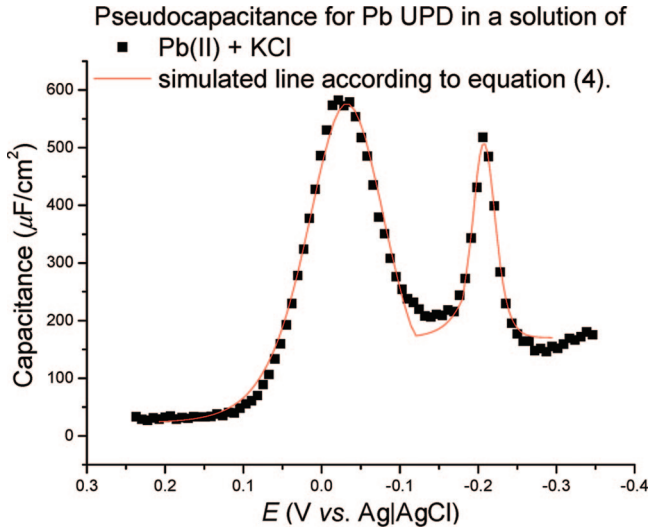

Figure 8. Dependence of the pseudocapacitance on the potential and its simulated line to fit the data shown in Figure 7b according to the Langmuir isotherm (eq 4).

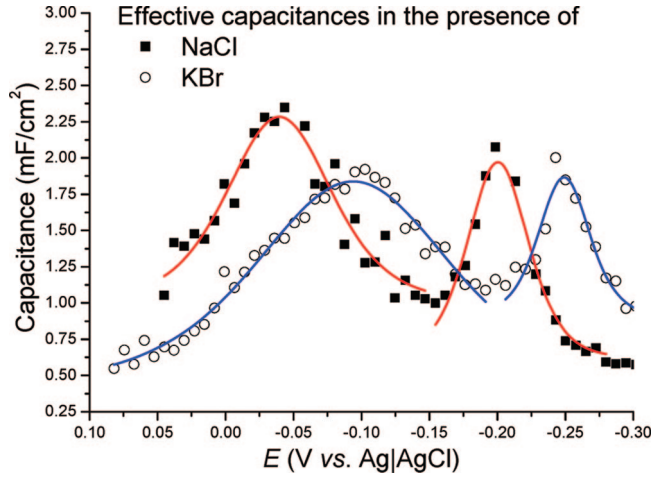

Figure 9. Effective capacitances calculated for the lead UPD obtained from CPEs (Q) using eq 7. The CPE values were obtained from the simulation of impedance data using equivalent circuit shown in Figure 4b.

The f values thus estimated were 5.9, 4.4, 4.4, and 4.8 with no additive, NaCl, KCl, and KBr present, respectively, for the first peak while they were −0.61, −0.60, −0.69, and −1.4 for the second peak. This indicates that the adsorbed Pb^{2+} ions repulse each other during the first stage of the UPD in the potential range of the first UPD peak in the presence of halide ions, whereas they weakly attract the other at the second stage. The decreasing f values for the first peaks in the presence of halides indicate that the presorbed halide ions help reduce the repulsion between Pb^{2+} ions on the surface during the first stage of the UPD due to their strong attraction of Pb^{2+} ions. Furthermore Br^- even increases the attraction of the Pb^{2+} at the second stage. From the mechanistic point of view, the presorbed anions attract the Pb^{2+} ions closer to the surface sites by Coulombic forces and are released upon charging the capacitor at the first stage when two-dimensional islands form and grow.[5b] On the other hand, specifically adsorbed Br^- in the space left unoccupied during the first stage plays an effective role of enhancing the attraction among the Pb^{2+} ions on the surface in the second stage, and the Pb atomic monolayer gets more compact by the collective interactions of the adsorbed metal ions and the vacancies of the monolayer are filled in by Pb atoms.

The effective capacitance of the system may be obtained simply by adding up the double-layer and pseudo capacitances when they are connected in parallel with no other elements.[21] However, the two capacitances cannot be simply summed up in our case because of the intervening resistor, R_{p1}, which causes a phase shift. We thus simplified the circuit shown in Figure 4a to a constant phase element (CPE), Q, as shown in Figure 4b. The CPE, which has been used for the interpretation of the Pb UPD process,[9b] represents the effective capacitance of the system well because it would have characteristics of both faradaic and nonfaradaic processes. Thus, the element Q of the alternative circuit shown in Figure 4b would represent an integrated value of C_{dl}, R_{p1}, and C_{φ}. The fitting of the impedance data to the circuit was excellent, from which values of Q and R_p were obtained. Then, effective capacitances were calculated from[25]

$$C_{eff} = \frac{(QR_p)^{1/n}}{R_p} \quad (7)$$

where n is a parameter defined in the CPE admittance, $Y = Y_{CPE}\omega^n \cos(2\pi/2) + jY_{CPE}\omega^n \sin(2\pi/2)$. The C_{eff} values thus obtained are plotted as a function of potential in Figure 9. Note that the C_{eff} vs E curves closely trace the voltammetric curves shown in Figures 1 and 2. The C_{eff} values at the peak potentials are also listed in Table 1, which are in excellent agreement with those obtained from the scan rate dependencies of the CV peak currents.

By use of eq 7, the charge required to form a monolayer was found to be 0.17, 0.25, 0.28, and 0.22 mC/cm^2 for the experiments with no halides, NaCl, KCl, and KBr present, respectively. The required charge for the full coverage of the lead UPD on gold surface was estimated to be 0.44 mC/cm^2 based on the number of atoms of the substrate per unit area.[22] Thus, the observed charges would account for only 39, 57, 64, and 50% of a monolayer, respectively, for the above solutions. The submonolayer coverage observed here confirms that a full monolayer adsorption of Pb^{2+} is not feasible on gold due to the larger diameter of Pb than that of a gold atom as reported in the literature.[6b]

Now the UPD can be described in terms of R_p, C_{dl}, and C_{φ}; the increase in the cathodic UPD current is thus made of those charging the double-layer capacitor, C_{dl}, and pseudocapacitor, C_{φ}, as well as overcoming the activation process, R_p. Lead ions adsorbed on the specifically adsorbed halide ions are reduced at the electrode causing the UPD currents to flow, leading to the Pb UPD. Thus, the strong electric field formed at the interface would accelerate the electron transfer during the Pb UPD.

To confirm the presorption of halide ions prior to the Pb UPD, experiments were conducted in the absence of Pb^{2+} with only halide ions present. Figure 10a shows the CVs in the absence and presence of 10 mM NaCl, in which the increased currents are observed due to desorption of adsorbed chloride ions upon charging the capacitor formed at the surface. The chloride is known to have an electrosorption valency of −0.8 at a single gold crystal surface.[26] This means that the chloride ion is adsorbed on the gold surface with an approximate stoichiometry of $Au^{-0.8}Cl^{-0.2}$ in this region, indicating that approximately 80% of its charge is transferred to the gold atom. This adsorption would take place on the positive side of the potential of zero charge (PZC), which should be near 0.03 V vs Ag|AgCl (in saturated KCl),[27] although exact values of both the electrosorption valency and the PZC depend on the crystallinity of the gold electrode and the electrolyte composition. Nevertheless, it

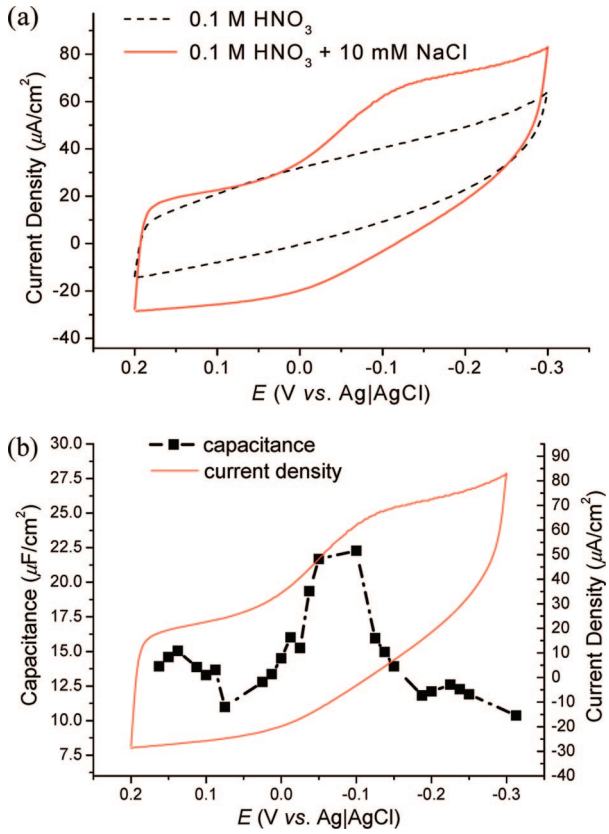

Figure 10. (a) CVs recorded at a gold electrode in 0.10 M HNO_3 solutions without (dashed line) and with (solid line) 10 mM NaCl in the absence of Pb^{2+} at a scan rate of 12.5 mV/s, and (b) the capacitances vs E plot obtained from impedance measurements.

is readily expected that the desorption of the presorbed chloride ions should occur by fully charging the capacitor formed across the double-layer near the PZC; this is shown as the enhanced current in Figure 10a. While the current peak is not as sharp as those observed at single crystal gold electrodes such as Au(111) due to the mixed crystallinity and the different electrolyte solutions used, the potential is in general in excellent agreement with those observed at Au(111).[26]

Impedance data were obtained in the same potential range with a blank solution containing only chlorides. The electrical double-layer capacitances obtained by fitting the impedance data to the equivalent circuit are plotted in Figure 10b along with the CV current. The changes in capacitance indicate the changes in the electrical double-layer formed, providing the direct information on the adsorption/desorption of chloride ions at the electrode. As shown in Figure 10b, the capacitance changes in the same manner as the current does during the lead UPD. It is noted that the maximum values of the capacitance appear near the potential where the first UPD peak currents are observed in the solution containing lead ions. This shows that the presorbed halide ions are present at a maximum amount when the UPD current approaches the peak value. The lead ions adsorbed on the top of the presorbed chlorides due to the strong chemical interaction as well as the increased Coulombic force should then be responsible for Pb UPD. This would lead to the observation of more distinctive voltammetric wave shapes in CVs and significantly large values of the electrical double-layer capacitance.

Now we can describe the mechanism for the Pb UPD in the presence of halide ions from our experimental results described thus far. The total negative charge of the electrode increases due to the specific adsorption of halide ions, which enhance the adsorption of Pb^{2+} at the electrode surface due to the chemical interaction as well as the Coulombic forces. The presorbed halide layer and Pb^{2+} on its top at the electrode surface form a pseudocapacitor to give more distinctive voltammetric wave shapes in CVs. Only fixed amounts of Pb^{2+} participate in the UPD reaction at given sites of the crystalline facets, inducing surface-confined electrochemistry. The bonds between Pb^{2+} and halides at the electrode surface are broken up upon electron transfer from the electrode according to the reaction

$$[Au^{-0.8}Cl^{-0.2}]^2(Pb^{2+}) + 2e^- \rightarrow 2AuPb + 2Cl^- \qquad (8)$$

releasing the adsorbed halides and reducing Pb^{2+} to Pb(0) upon charging the capacitor formed at the electrode surface. The formation of ion pairs between presorbed Cl^- and Pb^{2+} leading to a pseudocapacitor and the release of Cl^- from Pb(0) were also shown by XPS and EQCM experiments.[27] Once the part of the electrode is covered by the underpotentially deposited lead, it does not participate in a further UPD reaction on the Pb covered surface any more, causing the UPD currents to decrease until a new surface of unoccupied facets is available, where the second UPD takes place. The energy needed to break up the chemical bond between lead and halide and the adsorption energy of halide ions on the electrode account for most of the negative shifts observed in CVs.

Conclusion

In this work, real-time impedance measurements during Pb UPD have been carried out by employing the SCV-FTEIS technique during a single pass of the SCV experiment. The technique made it possible to monitor the changes in the electrode/electrolyte interface properties in real-time during the potential sweep. On the basis of the information thus obtained, we were able to work out the mechanism for the Pb UPD; the Pb UPD is described as the reduction of Pb^{2+} adsorbed on the presorbed anions. The Pb^{2+} adsorption is described by the Langmuir model at the beginning, which is taken up by the Frumkin adsorption when the population of adsorbates becomes high enough for them to interact with each other. Thus, the Pb UPD is described in terms of R_p, C_{dl}, and C_φ; the increase in the cathodic UPD current consists of those charging the double-layer capacitor, C_{dl}, and pseudocapacitor, C_φ, as well as overcoming the activation process, R_p. To our knowledge, this is the first attempt to elucidate the mechanism of the Pb UPD based on the information from the real time impedance measurements during the reaction. Our study clearly provides new insights into the Pb UPD process in the presence of halide ions, which would have been impossible had the novel real time SCV-FTEIS not been used. The study also offers an excellent example for demonstrating the power of the SCV-FTEIS technique in studying electrochemical processes as were the cases for studying a complex electrochemical reaction such as aniline oxidation[28] and the resolution of a one-step two electron transfer reaction into two.[29]

Acknowledgment. This work was supported by a grant from the KOSEF through the Center for Integrated Molecular Systems located at Postech (Grant No. R11-2000-070-070010) and the BK21 program.

References and Notes

(1) Schmickler, W. *Interfacial Electrochemistry*; Oxford: New York, 1996; pp 45−51.

(2) Budevski, E.; Staikov, G.; Lorenz, W. J. *Electrochemical Phase Formation and Growth*; VCH: Weinheim, 1996.

(3) Kolb, D. *M. Advances in Electrochemistry and Electrochemical Engineering*; Jone Wiley & Sons: New York, 1978; Vol. 11, p 125.

(4) Taguchi, S.; Aramata, A. *J. Electroanal. Chem.* **1998**, *457*, 73.

(5) (a) Engelsmann, K.; Lorenz, W. J.; Schmidt, E. *J. Electroanal. Chem.* **1980**, *114*, 11. (b) Ganon, J. P.; Clavilier, J. *Surf. Sci.* **1984**, *145*, 487. (c) Tao, N. J.; Pan, J.; Li, Y.; Oden, P. I.; DeRose, J. A.; Lindsay, S. M. *Surf. Sci.* **1992**, *271*, L338. (d) Hamelin, A.; Katayama, A. *J. Electroanal. Chem.* **1981**, *117*, 221. (e) Hamelin, A.; Lipkowski, J. *J. Electroanal. Chem.* **1984**, *171*, 317.

(6) (a) Engelsmann, K.; Lorenz, W. J.; Schmidt, E. *J. Electroanal. Chem.* **1980**, *114*, 1. (b) Kirowa-Eisner, E.; Bonfil, Y.; Tzur, D.; Gileadi, E. *J. Electroanal. Chem.* **2003**, *552*, 171. (c) Melroy, O.; Kanazawa, K.; Gordon II, J. G.; Buttry, D. *Langmuir* **1986**, *2*, 697. (d) Deakin, M. R.; Melroy, O. *J. Electroanal. Chem.* **1988**, *239*, 321.

(7) (a) Klimmeck, M.; Jüttner, K. *Electrochim. Acta* **1982**, *27*, 83. (b) Sackmann, J.; Bunk, A.; Pötzschke, R. T.; Staikov, G.; Lorenz, W. J. *Electrochim. Acta* **1998**, *43*, 2863.

(8) Lee, J.; Oh, I.; Hwang, S.; Kwak, J. *Langmuir* **2002**, *18*, 8025.

(9) (a) Ragoisha, G. A.; Bondarenko, A. S. *Electrochem. Commun.* **2003**, *5*, 392. (b) Bondarenko, A. S.; Ragoisha, G. A.; Osipovich, N. P.; Streltsov, E. A. *Electrochem. Commun.* **2005**, *7*, 631. (c) Garland, J. E.; Assiongbon, K. A.; Pettit, C. M.; Emery, S. B.; Roy, D. *Electrochim. Acta* **2002**, *47*, 4113.

(10) (a) Emery, S. B.; Hubbley, J. L.; Roy, D. *Electrochim. Acta* **2005**, *50*, 5659. (b) Pettit, C. M.; Goonetilleke, P. C.; Sulyma, C. M.; Roy, D. *Anal. Chem.* **2006**, *78*, 3723.

(11) (a) Yoo, J.-S.; Park, S.-M. *Anal. Chem.* **2000**, *72*, 2035. (b) Yoo, J.-S.; Park, S.-M. *Anal. Chem.* **2003**, *75*, 3294. (c) Chang, B.-Y.; Park, S.-M. *Anal. Chem.* **2006**, *78*, 1052. (d) Chang, B.-Y.; Hong, S.-Y.; Yoo, J.-S.; Park, S.-M. *J. Phys. Chem. B* **2006**, *110*, 19386. (e) Park, S.-M.; Yoo, J.-S. *Anal. Chem.* **2003**, *75*, 455A. (f) Park, S.-M.; Yoo, J.-S.; Chang, B.-Y.; Ahn, E.-S. *Pure Appl. Chem.* **2006**, *78*, 1069.

(12) Chang, B.-Y.; Park, S.-M. *Anal. Chem.* **2007**, *79*, 4892.

(13) (a) Gavaghan, D. J.; Elton, D.; Bond, A. M. *J. Electroanal. Chem.* **2001**, *513*, 73. (b) Zhang, J.; Guo, S.-X.; Bond, A. M.; Honeychurch, M. J.; Oldham, K. B. *J. Phys. Chem. B* **2005**, *109*, 8935. (c) Bond, A. M.; Duffy, N. W.; Guo, S.-X.; Zhang, J.; Elton, D. *Anal. Chem.* **2005**, 186A. (d) Baranski, A.; Szulborska, A. *J. Electroanal. Chem.* **1994**, *373*, 157. (e) Sher, A. A.; Bond, A. M.; Gavaghan, D. J.; Gillow, K.; Duffy, N. W.; Guo, S.-X.; Zhang, J. *Electroanalysis* **2005**, *17*, 15. (f) Fleming, B. D.; Barlow, N. L.; Zhang, J.; Bond, A. M.; Armstrong, F. A. *Anal. Chem.* **2006**, *78*, 2948.

(14) Application notes from www.ecochemie.nl provided by Eco Chemie.

(15) Budevski, E.; Staikov, G.; Lorenz, W. J. *Electrochemical Phase Formation and Growth*; VCH: Weinheim, Federal Republic of Germany, 1996; Chapter 3.

(16) Toney, M. F.; Gordon, J. G.; Samant, M. G.; Borges, G. L.; Melroy, O. R. *J. Phys. Chem.* **1995**, *99*, 4733.

(17) (a) Magnussen, O. M. *Chem. Rev.* **2002**, *102*, 679, and references therein. (b) Habib, M. A. In *Comprehensive Treatise of Electrochemistry*; Bockris, J. O'M.; Conway, B. E.; Yeager, E., Eds.; Plenum Press: New York, 1980; Vol. 1, pp 135−220. (c) Lipkowski, J.; Shi, Z.; Chen, A.; Pettinger, B.; Bilger, C. *Electrochim. Acta* **1998**, *43*, 2875.

(18) Lide, D. R. *CRC Handbook of Chemistry and Physics*, 74th ed.; CRC Press: Boca Raton, FL, 1993.

(19) Bard, A. J.; Faulkner, L. R. *Electrochemical Methods*, 2nd ed.; Wiley & Sons: New York, 2001; Chapters 5 and 10.

(20) Dean, J. A. *Lange's Handbook of Chemistry*, 13th ed.; McGraw Hill Book Company: New York, 1985.

(21) Srinivasan, S.; Gileadi, E. *Electrochim. Acta* **1966**, *11*, 321.

(22) Conway, B. E.; Gileadi, E. *Trans. Faraday Soc.* **1962**, *68*, 2493.

(23) Frumkin, A. N. *Z. Phys.* **1926**, *35*, 792.

(24) Dimitrov, N.; Vasilic, R.; Vasiljevic, N. *Electrchem. Solid State Lett.* **2007**, *10*, D79.

(25) Hsu, C. H.; Mansfeld, F. *Corrosion* **2001**, *57*, 747.

(26) Lipkowski, J.; Shi, Z.; Chen, A.; Pettinger, B.; Bilger, C. *Electrochim. Acta* **1998**, *43*, 2875.

(27) See, for example, Bockris, J. O'M.; Reddy, A. K. N.; Gamboa-Aldeco, M. *Modern Electrochemistry*, 2nd ed.; Kluwer Academic/Plenum Publishers: New York, 2000; Vol 2*A*, Chapter 6. The point of zero charge of gold is 0.23 V vs SHE in 0.02 N Na_2SO_4, which is about +0.03 V vs. Ag/AgCl (in saturated KCl) electrode used in this work.

(28) Hong, S.-Y.; Park, S.-M. *J. Phys. Chem. B* **2007**, *111*, 9779.

(29) Park, J.-B.; Chang, B.-Y.; Yoo, J.-S.; Hong, S.-Y.; Park, S.-M. *Bull. Korean Chem. Soc.* **2007**, *28*, 1523.

JP805960J